RESEARCH ARTICLE

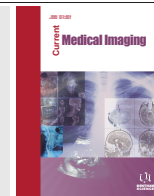# An Investigation Using Specific Absorption Rate Analysis to Diagnose Early-stage Breast Tumor using UWB Antenna

Rahul Krishnan[1,*] and Jobin Christ M.C[2]

[1]*Department of Electronics and Communication Engineering, Rajalakshmi Institute of Technology, Chennai, India;*
[2]*Department of Biomedical Engineering, Rajalakshmi Engineering College, Chennai, India*

Abstract: *Aims*: This work was focused on the detection of early-stage breast tumors and their location.

Background: The most frequently seen disease progression and mortality in women's lives is Breast Cancer. Because of breast cancer/tumors, the risk of mortality for women has risen exponentially. From the 2020 deadline for breast cancer, women who died from carcinoma were 123.8 cases per lac women between 2006-2010. This problem is also overcome by the early identification of the tumor using different detection procedures like X-ray mammography, computerized tomography, ultrasound imaging technique, Positron Emission Tomography (PET), Magnetic Resonance Imaging (MRI), microwave imaging. Researchers carried out multiple studies in these areas.

Objective: To detect early-stage breast tumors and their location using SAR analysis.

Methods: The major dielectrical difference between cancerous breast tissues and normal tissues in this technique is the microwave frequency range. The term Specific Absorption Rate (SAR) describes the amount of energy which is absorbed (W/kg) in the breast tissue. This segment illustrates the usefulness to diagnose the tumor position in the breast by means of maximum SAR value coordinates. Changes in breast and tumor size are important for the risk of diagnosis. The power absorbed in connecting with a normal breast and a tumor breast is measured and equivalent for different breast masses. The maximum SAR is also analyzed at distinct tumor locations at various frequency ranges.

Results: It is observed that max SAR coordinates are very close to the actual tumor location. So, the maximal value of SAR coordinates indicates the existence of a tumor in the breast phantom.

Conclusion: The simulated data above strongly suggests that the Max SAR values were higher in the breast phantom with tumor as compared to the breast without tumor. With different tumor radius (3 mm and 5 mm) analyzed with different resonant frequencies like 3GHz, 4GHz and 5GHz at the actual tumor location of (0, 0, 35). Even though a model representing the real properties of breast tissue is required to assess the validation of any imaging process, so the real-time development of an equivalent breast phantom and its execution is needed.

1. INTRODUCTION

The most frequently seen disease progression and mortality in women's lives is Breast Cancer. Because of breast cancer/tumors, the risk of mortality for women has risen exponentially. From the 2020 deadline for breast cancer, women who died from carcinoma were (123.8 per 100,000) women between 2006-2010. This problem is also overcome by the early identification of the tumor using different detection procedures like X-ray mammography, computerized tomography, ultrasound imaging technique, Positron Emission Tomography (PET), Magnetic Resonance Imaging (MRI), microwave imaging [1-6], researchers carried out multiple studies in these areas.

The X-ray imaging procedure is typically applied for the identification of the tumor, but the precise location of the tumor is very exorbitant and hard to locate. In addition, it will influence the healthful surrounding breast tissue [2]. An X-ray, in particular for women under the age of 40 years, cannot be replicated, due to its hazard [1, 7]. Ultrasound is a common tool for the diagnosis of breast cancer in the few mm range. They are distinguished from benign cysts, solid tumors, or suspicious cancers. It is very difficult to differentiate between malignant and benign tumors considering their vast abundance. Many micro-calcifications [8] are absent

*Address correspondence to this author at the Department of Electronics and Communication Engineering, Rajalakshmi Institute of Technology, Chennai, India; E-mail: rahulkrish1990@gmail.com

due to the speckle (hyperechoic spots). Another tool is MRI, which identifies the tumor sporty when compared to X-ray mammography's in women with inherited breast cancer susceptibility [9]. The MRI is used to classify problematic things such as benign and malignant lesions of the breast, leading to a more false-positive percentage [1, 4] which is costly and complex hardware is used. Such a limitation can be resolved by Microwave Imaging with UWB frequencies [10-12].

Microwaves are a favourable trade-off between resolution of the image and the penetration of wave deep inside the tissue and have recently been shown to distinguish the breast, in the UWB frequency range. This research shows the major dielectrical difference between cancerous breast tissues and normal tissues in this technique [4, 10, 13-15] in microwave frequency range. The term Specific Absorption Rate (SAR) describes the amount of energy which is absorbed (W/kg) in the breast tissue [16, 17]. The thermal distribution due to the interaction of electromagnetic wave with hemispherical breast phantom is analyzed based on Specific Absorption Rate (SAR) technique. SAR detects the abnormality in the human breast tissue. The energy associated with the electromagnetic wave is absorbed by the biological tissues, and this absorption of the electromagnetic field results in the heating of the human tissue. The heating effect of the tissue is normally quantified by the SAR. Even though SAR for breast tissue assessment may be too variable in an individual. The focus is given to the area where the maximum absorption is happening due to the presence of tumor. This segment illustrates the usefulness of diagnosing the tumor position in the breast by means of maximum SAR value coordinates. Changes in breast and tumor size are important for the risk of diagnosis. The power absorbed in connecting with a normal breast and a tumor breast is measured and equivalent for different breast masses. The maximum SAR is also analyzed at distinct tumor locations at various frequency ranges.

2. ANTENNA DESIGN

Different antennas with square-shaped ring slot [18], planar UWB antenna [19], UWB antenna in addition with CP-W-fed along with SRR loaded technique [20], Circular monopole antenna [21], antenna of dual band [22], MIMO antenna [23], monopole antenna in conjunction with printed circular disc [24] have been examined and their cons were used for the design of proposed antenna. Antenna design is done using CST Microwave Studio. The length of the rectangular patch 'L' is determined by using the frequency range of the system. The antenna length is calculated using the formula shown in equation (1):

$$L = \frac{1}{2 f_c \sqrt{\varepsilon_0 \varepsilon_r \mu_0}}$$ (1)

Where f_c is the center (resonant) frequency, is the relative permittivity of the substrate, is the permittivity in vacuum and A_0 is the permeability in vacuum.

In the microstrip antenna, width W of the patch controls the input impedance. The operating bandwidth can be increased by expanding the widths of the patch. The width 'W' is calculated using the equation (2):

$$W = \frac{c}{2 f_c} \sqrt{\frac{2}{\varepsilon_r + 1}}$$ (2)

f_c is the center (resonant) frequency, c is the speed of light and is the relative permittivity of the substrate [25].

The width is always adjusted in such a way that impedance matching occurs. And the length of the microstrip should be equal to I"/4. The ground and the patch layer are assembled using the copper material which is having a thickness of 0.035 mm. The substrate layer is assembled using the FR-4 lossy substance having the permittivity (ε_r = 4.3) having a height of 1.6 mm and the resulting antenna having a volumetric dimension of 43 x 40 x 1.6 mm³. Fig. (**1**) shows the evolution of the proposed UWB antenna from a basic rectangular patch with a Defected Ground Structure (DGS). Various dimensions used to design the proposed antenna which resonates at multiple frequencies are systemized in Table **1**. The proposed UWB antenna Geometry is highlighted in Fig. (**1b** and **c**).
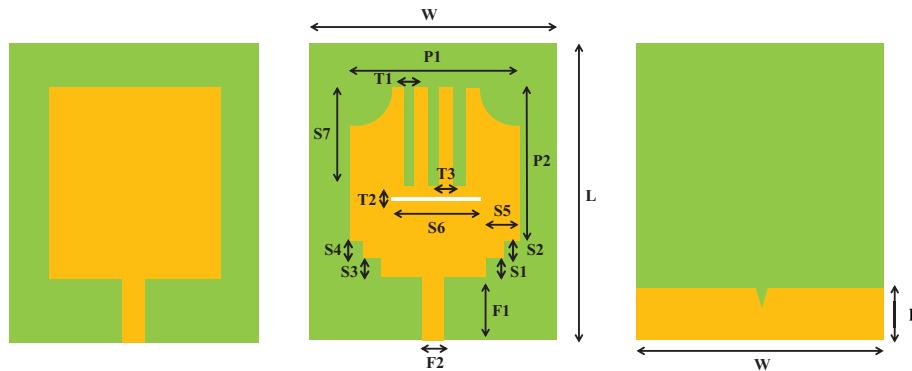

Fig. (1). Configuration of proposed UWB antenna (**a**) without slot (**b**) proposed (**c**) back perspective. (*A higher resolution / colour version of this figure is available in the electronic copy of the article*).

Table 1. Dimensions of proposed UWB antenna.

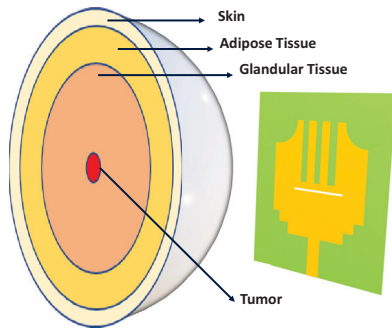| Parameter	Notation	Value (mm)
Length of substrate	L	40
Length of Patch	P1	25
Width of Patch	P2	24
Length of feed line	F1	10
Width of feed line	F2	3
Length of Ground	L'	8.6
Height of Patch	h1	0.035
Height of Substrate	h2	1.6
Height of Ground	h3	0.035
Width of three vertical slots	T1	1
Width of one horizontal slot	T2	0.5
Spacing between vertical slots	T3	1.5

Fig. (2). Experimental setup having heterogeneous breast phantom and proposed antenna. (*A higher resolution / colour version of this figure is available in the electronic copy of the article*).

3. DEVELOPMENT OF BREAST PHANTOM

The radius of the hemispherical breast phantom designed in CST Studio is 30 mm, which is placed at a distance of 70 mm away from the antenna. Heterogeneous breast phantom consists of multiple layers. The superficial layer is composed of skin. Generally, the thickness of the skin overlying the breast is about 2 mm thickness. Adipose tissues are present beneath the skin and are generally of thickness 5-20 mm. For phantom development, the thickness is considered

to be 8 mm. The remaining inner 20 mm thickness is composed of the fibro glandular tissue. The experimental setup with heterogeneous breast phantom and the proposed UWB antenna is shown in Fig. (**2**). The properties of the tissues that are used in the development of heterogeneous breast phantom are tabulated in Table **2**.

4. SPECIFIC ABSORPTION RATE (SAR)

The Specific Absorption Rate (SAR) is the derivative of the gradational energy (dW) which is held by a gradational mass (dm) found in an element of volume (dV) [26] which is expressed as:

$$SAR = \frac{d}{dt}(\frac{dW}{dm}) = \frac{d}{dt}(\frac{dW}{\rho dV})$$ (3)

The electric field can be correlated with SAR at a point by:

$$SAR = \frac{\sigma |E|^2}{\rho}$$ (4)

Where σ is the conductivity (Sm^{-1}), I? is the mass density (kgm^{-3}) and E is the electric field strength (Vm^{-1}). SAR is also defined as the Maximum Permissible Exposure (MPE) in the existence of the biological tissues in the fields of electromagnetics. It is expressed in Wkg^{-1}. SAR values are averaged for the entire body of 1g of tissue and 10g of tissue. Since this is a localized calculation of SAR, it is averaged over the tissue mass of 1g of tissue [27]. The various studies show that the early-stage detection of cancers is possible with SAR [28, 29]. Permissible SAR for humans under controlled and uncontrolled environments is tabulated in Table **3**.

5. RESULTS AND DISCUSSION

In this section, different antenna parameters like returning loss, gain, radiation pattern and the performance comparison of the proposed UWB antenna with the existing antenna are discussed. The analysis of averaged SAR values for 1g and 10g of tissue and coordinates in the heterogeneous breast without and with tumor at different frequencies are discussed.

Table 2. Properties of various tissues.

Tissue	Relative Permittivity	Electrical Conductance S m^{-1}	Density Kgm^{-3}	Heat Capacity Jkg^{-1}EsC^{-1}	Thermal Conductance Wm^{-1}EsC^{-1}
Skin	36.7	2.34	1109	3391	0.37
Adipose	4.84	0.262	911	2348	0.21
Glandular	50	3.46	1041	2960	0.33
Tumor	54.9	4	1058	-	-

Table 3. SAR Exposure Limits.

Environment	(Wkg^{-1})	SAR$_{1g}$ (Wkg^{-1})	SAR$_{10g}$ (Wkg^{-1})
Controlled	0.4	8	20
Uncontrolled	0.08	1.6	4

5.1. Antenna Parameter Analysis

In CST studio, hexahedral TLM solver setting is selected and the simulation is done with -40dB accuracy and 50Ω port impedance. Fig. (**3**) shows the comparison of S11 characteristics of the antenna without a slot and proposed one. The proposed UWB antenna produces a bandwidth whose frequency ranges from 2.5GHz to 13.5GHz which is quite remarkable.
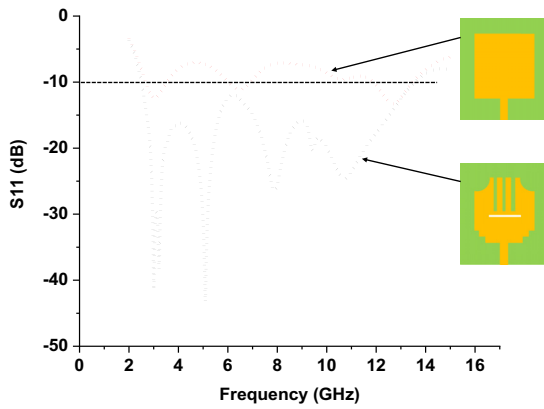

Fig. (3). S-parameter response of designed antenna. (*A higher resolution / colour version of this figure is available in the electronic copy of the article*).

The proposed antenna that resonates at two different frequencies nearly 3 GHz has a directivity of 2.507 dBi, gain of 2.076 dBi and 5 GHz has a directivity of 4.159 dBi, gain of 3.681 dBi. The gain *vs.* frequency plot in Fig. (**4**) clearly shows that there is not much variation in terms of gain between the initial design and the proposed antenna. But the bandwidth increases abruptly in the UWB range. The nor-

malized radiation pattern for H-plane (cut angle phi=90) and E-plane (cut angle phi=0) of proposed UWB antenna is displayed at frequency of 3GHz and 5GHz is exposed in Fig. (**5**).

5.2. Performance Comparison of Proposed Antenna with Existing Antennas

A comparison of the various antennas with respect to their area, frequencies, sizes, and bandwidths is presented in Table **4**. For various substrate materials, the proposed antenna is simulated and its effects are verified and differentiated along with various types of antennas, as exposed in Table **4**. The above-mentioned antennas have achieved wider width. Due to the invention of modern electronic technology, the size of the antenna is small whereas the bandwidth can be greater. The proposed UWB antenna has large bandwidth and smaller in size when compared to different antennas mentioned in Table **4**.
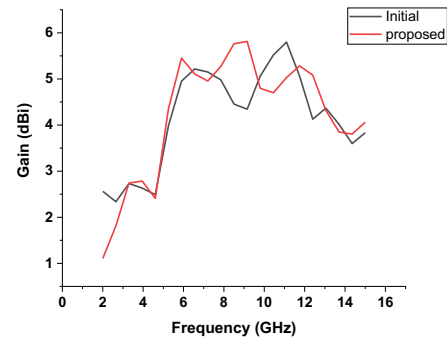

Fig. (4). Comparison of gain *vs.* frequency plot for initial design and proposed design. (*A higher resolution / colour version of this figure is available in the electronic copy of the article*).
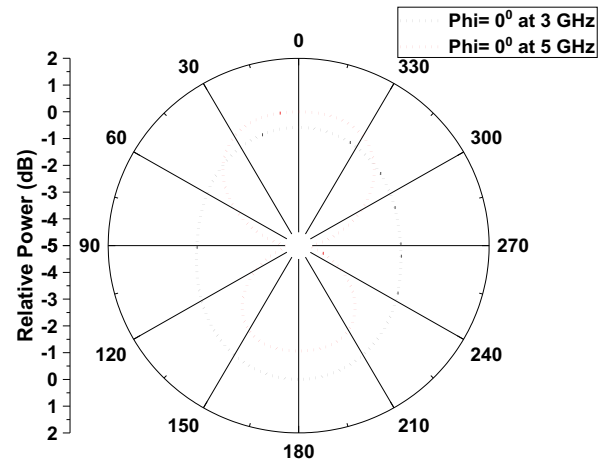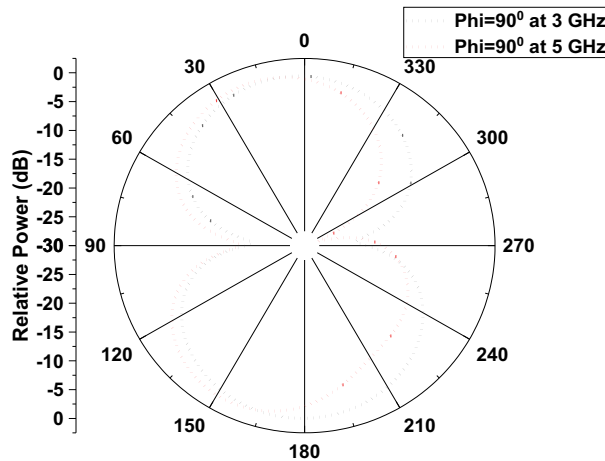

Fig. (5). Normalized radiation pattern at 3 GHz and 5 GHz (**a**) H-plane pattern (**b**) E-plane pattern. (*A higher resolution / colour version of this figure is available in the electronic copy of the article*).

Table 4. Comparison of proposed UWB antenna with existing antennas.

Refs.	Antenna Type	Freq. (GHz)	ABW (GHz)	FBW	Material	Area (LA-W)
[18]	Ring slot antenna	3-11	8	114.2%	RO4003B (ε_r = 3.4)	12000m^2
[19]	Planar UWB antenna	3.1-10.6	7.5	109.4%	RO4003 (ε_r = 3.38)	5850m^2
[20]	SRR-loaded UWB antenna	2.37-10.93	8.56	128.7%	Taconic (ε_r = 2.33)	2500m^2
[21]	Circular monopole antenna	2.6-10.8	8.2	122.3%	Taconic (ε_r = 2.33)	2500m^2
[22]	Dual band antenna	2.8-10.6	7.8	116.4%	FR4 ε_r = 4.6)	1720m^2
[23]	MIMO antenna for UWB	3.1-12	8.9	117.8%	FR4 (ε_r = 4.4)	1820m^2
[24]	Printed circular disc monopole	2.69-10.16	7.47	116.2%	FR4 (ε_r = 4.7)	2100m^2
[PA]	Slotted rectangular UWB antenna	2.5-13.5	11	137.5%	FR4 (ε_r =4.3)	1720m^2

Freq: Frequency, ABW: Absolute Bandwidth, FBW: Fractional Bandwidth, PA: Proposed Antenna.

Table 5. Averaged SAR values for 1g & 10g of tissue and coordinates in heterogeneous breast without tumor.

Frequency (GHz)	1 Gram Analysis			10 Gram Analysis		
	Maximum SAR W kg-1	Total SAR W kg-1	Maximum at (X, Y, Z) mm	Maximum SAR W kg-1	Total SAR W kg-1	Maximum at (X, Y, Z) mm
3	1.140	0.4805	(0.25, -8.75, 45.66)	0.7019	0.4814	(0.25, -5.06, 40.33)
4	0.899	0.3014	(0.25, 1.40, 40.33)	0.5184	0.3014	(0.25, 3.12, 40.33)
5	0.615	0.195	(0.25, 10.45, 46.33)	0.3415	0.1952	(0.25, 8.27, 51.47)

Table 6. Averaged SAR values for 1g & 10g of tissue and coordinates in heterogeneous breast with tumor of radius 3mm.

Frequency (GHz)	1 Gram Analysis			10 Gram Analysis		
	Maximum SAR W kg-1	Total SAR W kg-1	Maximum at (X, Y, Z) mm	Maximum SAR W kg-1	Total SAR W kg-1	Maximum at (X, Y, Z) mm
3	4.655	0.3070	(-0.12, -0.56, 20.2)	2.381	0.3070	(-0.12, -0.93, 31)
4	1.579	0.101	(0.12, 5.04, 20.25)	0.7787	0.101	(-0.12, 2.35, 31)
5	1.288	0.072	(-0.12, 11, 25.46)	0.559	0.072	(-0.12, 10.53, 31.4)

Table 7. Averaged local SAR values and coordinates for 1g & 10g of tissue in heterogeneous breast for the tumor of radius 5mm.

Frequency (GHz)	1 Gram Analysis			10 Gram Analysis		
	Maximum SAR W kg-1	Total SAR W kg-1	Maximum at (X, Y, Z) mm	Maximum SAR W kg-1	Total SAR W kg-1	Maximum at (X, Y, Z) mm
3	4.727	0.314	(0.12, -0.93, 20.25)	2.416	0.314	(-0.12, -1.31, 31.04)
4	1.577	0.101	(0.12, 5.21, 20.25)	0.776	0.101	(-0.12, 2.29, 31.04)
5	1.289	0.072	(-0.12, 11, 25.46)	0.559	0.072	(-0.12,10.53,31.45)

5.3. Analysis of Averaged SAR Values in Heterogeneous Breast

Heterogeneous breast phantom is radiated using an UWB signal from the proposed antenna. Maximum SAR, Total SAR and coordinates of Maximum SAR are obtained for the resonant frequency of 3, 4 and 5 GHz respectively. Table **5** reflects total, Maximum SAR and the coordinate values of a breast phantom without tumor in 1g and 10g analysis. Similarly, Tables **6** and **7** show values of total Maximum SAR and the coordinate Maximum SAR of a breast phantom with tumor of radii 3 mm and 5 mm respectively placed at a coordinate location (0, 0, 35). It is clearly seen that the maxi-

mum SAR is always higher in breast phantom with tumor as compared to without a tumor in all three frequency ranges, which is clearly shown in Fig. (**6**). By verifying the Maximum SAR coordinate value of the phantom with and without tumor, it is observed that the coordinate values of tumor with 3 mm radius at 3, 4 and 5 GHz frequency is approximately near to the actual tumor location (0, 0, 35) which clearly shows the presence of the tumor and its location.

By analyzing the 1Gram SAR analysis and 10Gram SAR analysis, the phantom along with tumor of radii like 3mm and 5 mm is shown in Tables **6** and **7**. For 1Gram analysis, the coordinate obtained for 3 mm tumor at 3 GHz is

(-0.12, -0.56, 20.2) and the coordinate obtained for 5 mm tumor at 3 GHz is (0.12, -0.93, 20.25). But for 10Gram analysis, the coordinate obtained for 3 mm tumor at 3 GHz is (-0.12, -0.93, 31) and the coordinate obtained for 5 mm tumor at 3 GHz is (-0.12, -1.31, 31.04). From the above observation, the tumor location detection is more accurate in 10-Gram analysis with the actual tumor location of (0, 0, 35).

Furthermore, the SAR analysis was carried out for different tumor locations at 5 mm and 3 mm radius tumor. In the case of different tumor locations, Maximum SAR for 3 mm and 5 mm radius tumors remains almost the same. The coordinate location of Maximum SAR at 3 mm and 5 mm tumors is very much nearer to the actual tumor location, as shown in Fig. (**7**).
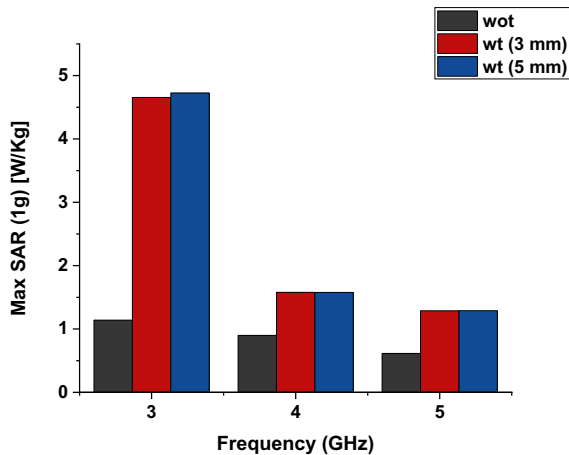

Fig. (6). Comparison of maximum SAR value for various frequencies in without and with tumor breast. (*A higher resolution / colour version of this figure is available in the electronic copy of the article*).
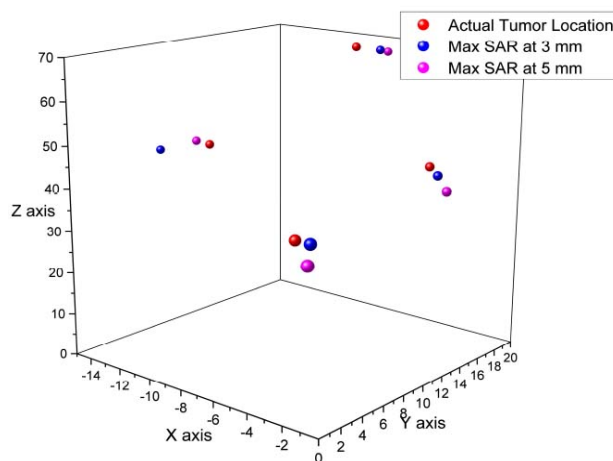

Fig. (7). Comparison of various positions of actual, maximum SAR at 5mm and 3mm tumor radius. (*A higher resolution / colour version of this figure is available in the electronic copy of the article*).

CONCLUSION

A compact slotted rectangular UWB antenna is proposed for the early-stage detection of the breast tumor using SAR analysis. The proposed compact antenna successfully brings out a bandwidth of 2.5GHz to 13GHz. The simulated data above strongly suggests that the maximum SAR values were higher in the breast phantom with tumor as compared to the breast without tumor. With different tumor radius (3 mm and 5 mm) analyzed with different resonant frequencies like 3,4 and 5GHz at the actual tumor location of (0, 0, 35). It is observed that maximum SAR coordinates are very close to the actual tumor location. So, the maximal value of SAR coordinates indicates the existence of a tumor in the breast phantom. Even though a model representing the real properties of breast tissue is required to assess the validation of any imaging process, so the real-time development of an equivalent breast phantom and its execution is needed.

ETHICS APPROVAL AND CONSENT TO PARTICIPATE

Not applicable.

HUMAN AND ANIMAL RIGHTS

No animals/humans were used for studies that are the basis of this research.

CONSENT FOR PUBLICATION

Not applicable.

AVAILABILITY OF DATA AND MATERIALS

Not applicable.

CONFLICT OF INTEREST

The authors declare no conflict of interest, financial or otherwise.

REFERENCES

[1]   Wang J, Chen H, Wu X, *et al.* Comparison of diagnostic efficiency of breast cancer imaging in Chinese women: Digital mammography, ultrasound, MRI, and combinations of these modalities. J Med Imaging Health Inform 2015; 5(7): 1488-93.
http://dx.doi.org/10.1166/jmihi.2015.1564
[2]   AlShehri SKSA. UWB imaging for breastr cancer detection using neural network. Prog Electromagn Res C 2009; 7: 79-93.
http://dx.doi.org/10.2528/PIERC09031202
[3]   Williams T, Fear EC, Westwick DW. Tissue sensing adaptive radar for breast cancer detection: Investigations of reflections from the skin. IEEE Antennas Propag Soc AP-S Int Symp 2004; 3: 2436-9.
http://dx.doi.org/10.1109/APS.2004.1331865
[4]   Selvaraj V, Sheela JJ, Krishnan R, *et al.* Detection of depth of the

tumor in microwave imaging using ground penetrating radar algorithm. Prog Electromagn Res M 2020; 96: 191-202.
http://dx.doi.org/10.2528/PIERM20062201

[5]   Yifan C, Gunawan E, Yongmin K, *et al.* UWB microwave imaging for breast cancer detection: Tumor/clutter identification using a time of arrival data fusion method. IEEE Antennas Propag Soc AP-S Int Symp 255-8.2006; NM, USA.
http://dx.doi.org/10.1109/APS.2006.1710504

[6]   Fear EC, Li X, Hagness SC, Stuchly MA. Confocal microwave imaging for breast cancer detection: Localization of tumors in three dimensions. IEEE Trans Biomed Eng 2002; 49(8): 812-22.
http://dx.doi.org/10.1109/TBME.2002.800759 PMID: 12148820

[7]   Shao W, Adams RS. UWB microwave imaging for early breast cancer detection: A novel confocal imaging algorithm IEEE Antennas Propag Soc AP-S Int Symp. vol. 2: 707-9.

[8]   Huo Y, Bansal R, Zhu Q. Breast tumor characterization *via* complex natural resonances. IEEE MTT-S Int Microw Symp Dig 2003; 1: 387-90.
http://dx.doi.org/10.1109/MWSYM.2003.1210958

[9]   Kriege M, Brekelmans CT, Boetes C, *et al.* Efficacy of MRI and mammography for breast-cancer screening in women with a familial or genetic predisposition. N Engl J Med 2004; 351(5): 427-37.
http://dx.doi.org/10.1056/NEJMoa031759 PMID: 15282350

[10]   Joselin Jeya Sheela J, Vanaja S. Novel directional antennas for microwave breast imaging applications Int Conf Smart Electron Commun 2020; 599-603.
http://dx.doi.org/10.1109/ICOSEC49089.2020.9215243

[11]   Nair Bindu G, Abraham S, Lonappan A, *et al.* Active microwave imaging for breast cancer detection. Prog Electromagn Res 2006; 58: 149-69.

[12]   Adnan S, Abd-Alhameed R, See C, *et al.* A compact UWB antenna design for breast cancer detection. Piers Online 2010; 6: 129-32.
http://dx.doi.org/10.2529/PIERS091029055334

[13]   Selvaraj V, Baskaran D, Rao PH, *et al.* Breast tissue tumor analysis using wideband antenna and microwave scattering. J Inst Electron Telecommun Eng 2018; 67: 49-59.
http://dx.doi.org/10.1080/03772063.2018.1531067

[14]   Selvaraj V, Srinivasan P, Jegadish KKJ, *et al.* Highly directional microstrip ultra wide band antenna for microwave imaging system. Acta Graph Znan časopis za Tisk i Graf Komun 2017; 28(1): 35-40.
http://dx.doi.org/10.25027/agj2017.28.v28i1.122

[15]   Selvaraj V, Srinivasan P, Baskaran D, *et al.* Characterisation of breast tissue using compact microstrip antenna. Int J Biomed Eng Technol 2019; 31(2): 161-75.
http://dx.doi.org/10.1504/IJBET.2019.102121

[16]   Shahira Banu MA, Vanaja S, Poonguzhali S. UWB microwave detection of breast cancer using SAR. 2013 Int Conf Energy Effic Technol Sustain ICEETS 2013. 113-8.

http://dx.doi.org/10.1109/ICEETS.2013.6533366

[17]   Selvaraj V, Srinivasan P. Interaction of an EM wave with the breast tissue in a microwave imaging technique using an ultra-wideband antenna. Biomed Res (Aligarh) 2017; 28(3): 1025-30.

[18]   Sadat S, Fardis M, Geran F, *et al.* A compact microstrip squaring-ring slot antenna for UWB applications. 2006 IEEE Antennas Propag Soc Int Symp. 4629-32.
http://dx.doi.org/10.1109/APS.2006.1711670

[19]   Mehdipour A, Mohammadpour-Aghdam K, Faraji-Dana R. A new planar ultra wideband antenna for UWB applications. 2007 IEEE Antennas and Propagation Society International Symposium. Honolulu, HI, USA. 2007; pp. 5127-30.
http://dx.doi.org/10.1109/APS.2007.4396700

[20]   Peng H, Wang C, Zhao L, *et al.* Novel SRR-loaded CPW-fed UWB antenna with wide band-notched characteristics. Int J Microw Wirel Technol 2017; 9(4): 875-80.
http://dx.doi.org/10.1017/S1759078716000702

[21]   Siddiqui JY, Saha C, Antar YMM. Compact SRR loaded UWB circular monopole antenna with frequency notch characteristics. IEEE Trans Antenn Propag 2014; 62(8): 4015-20.
http://dx.doi.org/10.1109/TAP.2014.2327124

[22]   Yassen M T, Ali J K, Hussan M R, *et al.* Extraction of dual-band antenna response from UWB based on current distribution analysis extraction of dual-band antenna response from UWB based on current distribution analysis. 2016.

[23]   Naser S, Dib N. Analysis and design of MIMO antenna for UWB applications based on the super-formula. Int Conf Electron Devices, Syst Appl 2017; 7-9.

[24]   Liang J, Chiau CC, Chen X, *et al.* Study of a printed circular disc monopole antenna for UWB systems. IEEE Trans Antenn Propag 2005; 53(11): 3500-4.
http://dx.doi.org/10.1109/TAP.2005.858598

[25]   Selvaraj V, Srinivasan P, Krishnan R. A compact UWB antenna for IEEE802.11a standard communication system. Int J Control Theory Appl 2016; 9(5): 2363-8.

[26]   IEEE Standards Coordinating Committee, I. S. C. C. 28, and IEEE Standards Coordinating Committee. IEEE Recommended Practice for Measurements and Computations of Radio Frequency Electromagnetic Fields with Respect to Human Exposure to Such Fields 2002; 2363-8.

[27]   IEEE standard for safety levels with respect to human exposure to radio frequency electromagnetic fields, 3 kHz to 300 GHz. IEEE Std C951-1991 1992; 1-76.

[28]   Kumari V, Sheoran G, Kanumuri T. SAR analysis of directive antenna on anatomically real breast phantoms for microwave holography. Microw Opt Technol Lett 2020; 62(1): 466-73.
http://dx.doi.org/10.1002/mop.32037

[29]   Dagheyan AG, Molaei A, Obermeier R, Martinez-Lorenzo J. Preliminary imaging results and SAR analysis of a microwave imaging system for early breast cancer detection. Proc Annu Int Conf IEEE Eng Med Biol Soc EMBS 2016; 1066-9.
http://dx.doi.org/10.1109/EMBC.2016.7590887